Photon energy dependence of photoneutron production from heavy targets

Thuong T.H. Nguyen[1,*], *Toshiya* Sanami[1,2], *Hirohito* Yamazaki[1,2], *Eunji* Lee[1,2], *Kenta* Sugihara[1,2], *Toshiro* Itoga[3], *Yoichi* Kirihara[4], *Shuji* Miyamoto[5], *Satoshi* Hashimoto[6], and *Yoshihiro* Asano[2,7]

[1]SOKENDAI, Shonan Village, Hayama, Kanagawa 240-0193, Japan
[2]KEK, 1-1 Oho, Tsukuba-shi, Ibaraki-ken 305-0801, Japan
[3]JASRI, 1-1-2, Kouto, Kamigori-cho, Ako-gun, Hyogo 678-1205, Japan
[4] JAEA, 2-4 Shirakata, Tokai-mura, Naka-gun, Ibaraki 319-1195, Japan
[5] ILE, Osaka University, 2-6 Yamadaoka, Suita, Osaka 565-0871, Japan
[6]University of Hyogo, 1-1-2, Kouto, Kamigori-cho, Ako-gun, Hyogo 678-1205, Japan
[7]RCNP, Osaka University, 10-1, Mihogaoka, Ibaraki, Osaka 567-0047, Japan

Abstract. The double differential cross-sections (DDXs) of photoneutron production via the photonuclear reaction on tantalum, tungsten, and bismuth for 13 and 17 MeV linearly polarized photon beams were measured using the time-of-flight method at the NewSUBARU-BL01 facility. Polarized photons were obtained by the Laser Compton backscattering (LCS) technique. Two distinct components were observed on the spectra: the low-energy component up to 4 MeV and the high-energy above 4 MeV. The angular distribution of the low-energy component was isotropic, whereas the high-energy was distributed anisotropically and influenced by the angle between direction of photon polarization and neutron emission, especially for 17 MeV photon energy. These phenomena were similar to those of ^{197}Au target observed in the previous studies. The low-energy neutron distributions at 13 and 17 MeV photon energies were almost identical for all three targets. The DDX energy integration was calculated and compared among the three targets for two-photon energies. Given the horizontal polarization (plane parallel to the x-axis) of the incident photons, the emission angles of 90° on the x-axis and y-axis recorded the maximum and minimum photoneutron yield, respectively. The differences between these two positions were minor for ^{181}Ta and ^{nat}W at 13 MeV photon energy and noticeable for other cases. An underestimation of the TENDL nuclear data library was observed on the photoneutron DDXs compared to the experimental results for ^{181}Ta and ^{209}Bi.

1 Introduction

Yield, energy, and angular distribution of photoneutron via photonuclear reaction, is a fundamental concern for shielding design in electron accelerators and understanding the nuclear reaction mechanism. In electron accelerators, secondary neutrons, called

* e-mail: ngthuong@post.kek.jp

photoneutrons, are emitted from the interaction between photons as bremsstrahlung and accelerator components.

So far, the photoneutron yield is usually obtained from experimental reaction cross-section data available on the EXFOR library [1]. In contrast, there is a comparative dearth of experimental knowledge concerning energy and angular distribution, which mainly rely on the existing theoretical nuclear reaction models for calculating cross-section data.

Along with the development of the laser Compton backscattering (LCS) technique [2] producing a high-intensity monoenergetic polarized photon beam, Kirihara et al. [3] and Tuyet et al. [4] studied photoneutron energy spectra on medium and heavy targets using 16.6 MeV linearly polarized photons. The observed spectra exhibited two primary components: a low-energy evaporation component with an isotropic distribution (below 4 MeV) and a high-energy direct component exhibiting an anisotropic distribution (above 4 MeV). Notably, the yield of high-energy photoneutrons correlated with the angle between the direction of photon polarization and neutron emission. These studies provided valuable data for understanding particle emission via photonuclear reactions.

Based on the experimental conditions stated in [3, 4], tantalum, tungsten, and bismuth were selected for photoneutron production's double differential cross-section (DDX) measurements at 17 and 13 MeV linearly polarized photons. This effort aims to enhance the existing database of photoneutron energy and angular distribution and further our understanding of the dependence on photon energy. These nuclei have similar reaction Q-values, cross-sections, and mass numbers. The DDX data are also essential for shielding design in electron accelerators. These nuclei, especially ^{181}Ta and ^{nat}W, are frequently employed in electron accelerators as material for collimators and targets due to their high atomic number, short radiation length, and high melting points. Consequently, the measured DDX data will be compared with the TENDL-2021 nuclear data library [5] to assess the adequacy of current theoretical nuclear models in simulating photonuclear reactions.

2 Experiment

Our experiments were carried out at the NewSUBARU facility, BL-01, Hyogo, Japan. The 13 and 17 MeV horizontally polarized photon beams were produced by the collision between 860.8 and 982.4 MeV electrons, respectively, in the storage ring and a polarized laser source at the backscattering angle. Figure 1 indicates the photon spectra obtained via a simulation calculation using EGS code [6]. The average energies were respectively 12.7 and 16.6 MeV. The photon beam intensity was approximately 10^5 photon/s.

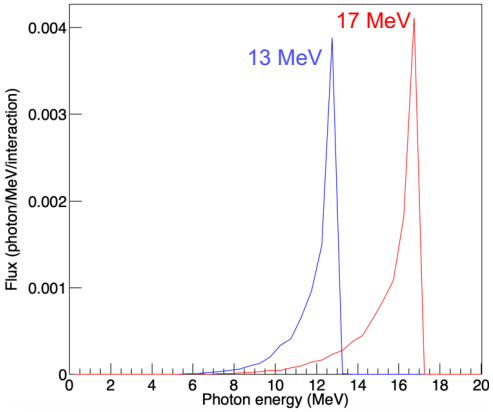

Fig. 1. LCS photon spectra.

Figure 2 shows the experimental setup of the photoneutron measurement, as mentioned in [4]. After being generated by the LCS technique, the photon beams were aligned to inject into the center of the target. Targets were cylinders with 1 cm thicknesses for ^{181}Ta and ^{nat}W and 2 cm for ^{209}Bi. A 5-mm-thick plastic scintillator was placed upstream of the target to estimate the number of incident photons. Six liquid scintillation detectors NE213, each 127 mm in diameter and 127 mm in thickness, were positioned at 30°, 60°, 90°, 120°, and 150° horizontally and 90° vertically with respect to the photon beam direction. The pulse shape discrimination (PSD) technique was used to reject secondary gamma rays against neutrons. The time-of-flight (TOF) method was applied to obtain the photoneutron energy spectra.

DDXs of photoneutron production were obtained from the neutron counting spectra

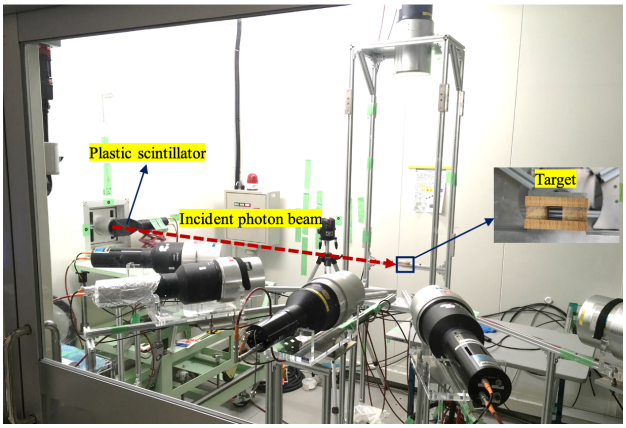

Fig. 2. Experimental setup of the photoneutron measurement.

normalized by the number of incident photons, neutron detection efficiency, the number of target atoms, and the solid angle and corrected by the attenuation of photon and neutron in targets. Neutron events with a light yield greater than 0.1 and 0.25 MeVee were selected for 13 and 17 MeV photons, respectively. The neutron detection efficiency of the detectors was calculated using the SCINFUL-QMD simulation [7] with correction of the neutron measurement from the ^{252}Cf source.

3 Results and Discussions

3.1 DDX of photoneutron production

Figure 3 shows DDX results of the (γ, xn) reaction on ^{181}Ta, ^{nat}W, and ^{209}Bi targets for 13 and 17 MeV horizontally polarized photons at six angles (30°, 60°, 90°, 120°, and 150° horizontal and 90° vertical). The six neutron detectors were labelled as H30, H60, H90, H120, H150, and V90, respectively. The measured photoneutrons range from 1.2 MeV to 6 MeV for 13 MeV photons and 2 MeV to 10 MeV for 17 MeV photons.

The DDX exhibited two distinct components: one occupied the energy realm below 4 MeV, and the other representing high-energy neutrons. The energy and angular distribution of the low-energy component below 4 MeV appear nearly isotropic and

resemble the tail of the Maxwellian distribution. This isotropic distribution is attributed to neutron emission through the evaporation process [8].

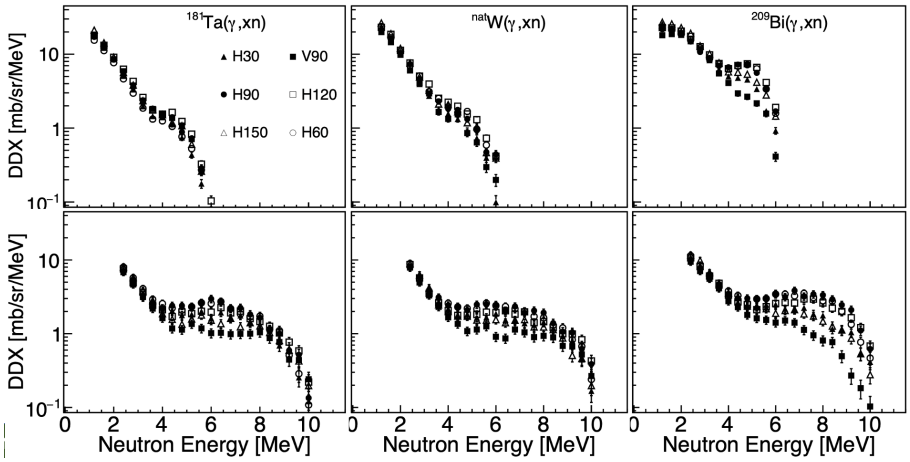

Fig. 3. DDXs of photoneutron production on ^{181}Ta, ^{nat}W, and ^{209}Bi at 13 MeV and 17 MeV photon energies.

Neutrons in the high-energy component are typically produced through the pre-equilibrium process [9] and influenced by the direction of photon polarization [3]. The pre-equilibrium process is described by the exciton model [10], where the incident particle creates complex states of excited particles and holes in the compound nucleus. However, nucleon particle emission during the pre-equilibrium has not been studied extensively for photonuclear reactions because of the lack of that kind of experimental data. Given the horizontal polarization of the incident photons, the H90 detector position recorded the maximum neutron yield, while the V90 position observed the least. For 17 MeV photons, neutron emission was highly dependent on the detector angle because of the incident photons' polarization direction. This observation mirrored a phenomenon reported by Kirihara et al. [3] observed with ^{197}Au targets at the same photon energy. Nonetheless, the polarization effect was insignificant for 13 MeV photons interacting with ^{181}Ta and ^{nat}W targets. Consequently, the differences in DDX values across emission angles for these targets and energy were minimal. More detailed analyses of the two components will be in the following sections.

3.2 Low-energy component

To analyze the low-energy component, the DDXs below 4 MeV were fitted to the Maxwellian distribution, the expression of which is as follows [8]:

$$\frac{dN}{dE}_{evap} = C\frac{E}{T^2}e^{-E/T} \quad (1)$$

where C denotes the multiplying factor, E (MeV) denotes the neutron energy, and T (MeV) denotes the nuclear temperature specializing for each nucleus.

Figure 4 shows the fitting of experimental data on ^{181}Ta, ^{nat}W, and ^{209}Bi for 13 MeV and 17 MeV photon energies at H120 emission angle with the Maxwellian function plotted as solid red lines. The average values of nuclear temperature on ^{181}Ta, ^{nat}W, and ^{209}Bi for 13 and 17 MeV photon energies are detailed in Table 1. The uncertainties of average values express the variation in temperature between the emission angles. The nuclear temperatures for 13 MeV and 17 MeV photons are closely identical. The slight difference in temperature between the two cases of photon energies was due to the fewer data points on the spectra for 17 MeV photons. Hence, the slope of the evaporation spectra remained almost identical between the photon energies of 13 and 17 MeV.

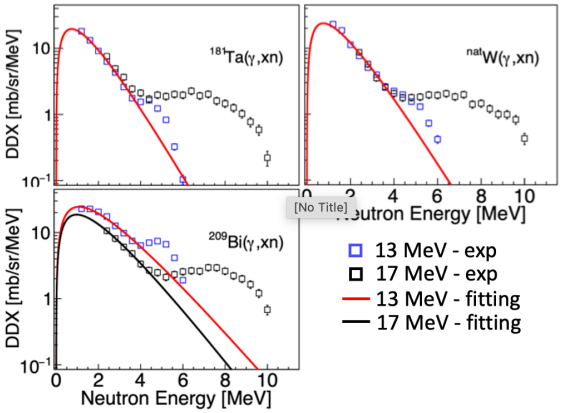

Fig. 4. Maxwellian fitting for photoneutron data on ^{181}Ta, ^{nat}W, and ^{209}Bi for 13 MeV and 17 MeV photon energies at H120 emission angle.

Table 1. Nuclear temperature parameters (MeV) of Maxwellian distribution for all the targets for 13 and 17 MeV photon energies.

Photon energy	^{181}Ta	^{nat}W	^{209}Bi
13 MeV	0.70 ± 0.03	0.71 ± 0.04	1.03 ± 0.06
17 MeV	0.87 ± 0.06	0.85 ± 0.09	0.96 ± 0.05

3.3 High-energy component

Table 2 lists the numerical values of the high-energy component's DDX energy integration, denoted as ADX, for 13 and 17 MeV photon energies at H90 and V90 emission angles, the recorded maximum and minimum high-energy photoneutron yield, respectively. ADX values on ^{181}Ta and ^{nat}W are always comparable, regardless of emission angles and photon energies. These are smaller than those on ^{209}Bi for both energies of photons. In other words, fewer high-energy photoneutrons are produced on ^{181}Ta and ^{nat}W targets.

The difference in ADX values between the emission angles implies the impact of photon polarization's direction on photoneutron emission. For 17 MeV photon energy, this difference between the H90 and V90 emission angles is relatively significant on all three targets. For 13 MeV photon energy, the gap between H90 and V90 is minor on ^{181}Ta and ^{nat}W but remains largely on ^{209}Bi.

Table 2. DDX energy integration (mb/sr) of the high-energy component for all the targets for 13 and 17 MeV photon energies at H90 and V90 emission angles.

Photon energy	13 MeV		17 MeV	
	H90	V90	H90	V90
^{181}Ta	1.33 ± 0.06	1.07 ± 0.05	10.64 ± 0.36	5.48 ± 0.21
^{nat}W	1.97 ± 0.09	1.41 ± 0.08	10.65 ± 0.35	5.46 ± 0.20
^{209}Bi	10.06 ± 0.37	3.90 ± 0.17	16.65 ± 0.52	6.52 ± 0.25

3.4 DDX comparison between experimental data and TENDL nuclear data library for ^{181}Ta and ^{209}Bi

Figure 5 displays the DDX spectra by experiment and TENDL nuclear data library for ^{181}Ta and ^{209}Bi at 13 and 17 MeV photon energies. The full and open red circle points are the experimental data at H90 and V90, the maximum and minimum high-energy photoneutron yield, respectively. The solid black lines indicate the DDX spectra by TENDL. This comparison suggests the underestimation of the TENDL nuclear data library toward the experimental results, even at the emission angles of V90, minimum photoneutron yield.

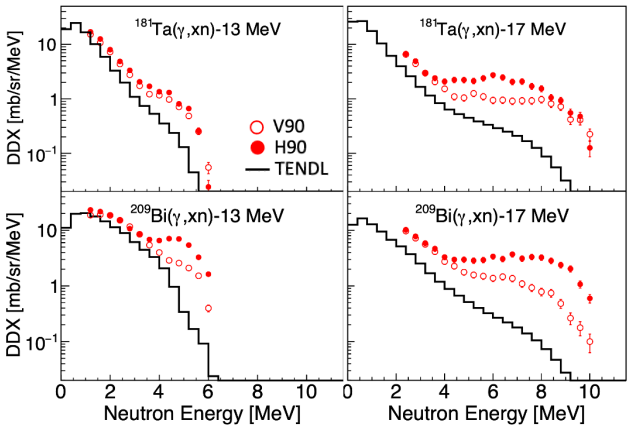

Fig. 5. DDX spectra by experiment and TENDL nuclear data library for ^{181}Ta and ^{209}Bi at 13 and 17 MeV photon energies.

4 Conclusion

The DDX data of photoneutron production on ^{181}Ta, ^{nat}W, and ^{209}Bi targets for 13 and 17 MeV linearly polarized photons suggested some characteristics in terms of photon energy dependence. Photoneutron emission below 4 MeV, the low-energy component, distributed isotropically. The slopes of this component for all targets were found to be comparable at the two energies of photons. The higher photoneutrons were recorded with anisotropic distribution. The anisotropic distribution was noticeable in almost all cases of photon energies and targets, but not for ^{181}Ta and ^{nat}W targets at 13 MeV photon energy. An underestimation of the TENDL nuclear data library toward the experimental results was observed when comparing two sets of results for ^{181}Ta and ^{209}Bi.

References

[1] N. Otuka, E. Dupont, V. Semkova, B. Pritychenko, A.I. Blokhin, M. Aikawa, S. Babykina, M. Bossant, G. Chen, S. Dunaeva, R.A. Forrest, Nuclear Data Sheets, **120**, 272-276 (2014)

[2] Y. Asano, S. Miyamoto, and LEPS-II collaboration, Prog. Nucl. Sci. Tech., **4**, 252 (2014)

[3] Y. Kirihara, H. Nakashima, T. Sanami, Y. Namito, T. Itoga, S. Miyamoto, A. Takemoto, M. Yamaguchi, Y. Asano, J. Nucl. Sci. Technol., **57**(4), 444-456 (2020)

[4] T.K. Tuyet, T. Sanami, H. Yamazaki, T. Itoga, A. Takeuchi, Y. Namito, S. Miyamoto, Y. Asano, Nucl. Instrum. Meth. A, **989**, 164965 (2021)

[5] A.J. Koning, D. Rochman, J. Sublet, N. Dzysiuk, M. Fleming and S. van der Marck, Nuclear Data Sheets ,**155**, 1-55 (2019)

[6] H. Hirayama, Y. Namito, W.R. Nelson, A.F. Bielajew, S.J. Wilderman, & U. Michigan, *The EGS5 code system* (No. SLAC-R-730), Department of Energy, United States (2005)

[7] D. Satoh, S. Kunieda, Y. Iwamoto, N. Shigyo, K. Ishibashi, J. Nucl. Sci. and Technol., **39**, 657-660 (2002)

[8] D.B. Gayther and P.D. Goode, J. of Nucl. Energy 21(9), 733–747 (1967)

[9] M.B. Chadwick and P.G. Young., Acta Physica Slovaca, **45**, 633– 644 (1995)

[10] A.J. Koning and M. C. Duijvestijn., Nuclear Physics A, **744**, 15-76 (2004)